



ELSEVIER

Journal of Chromatography A, 716 (1995) 241–257

JOURNAL OF  
CHROMATOGRAPHY A

## Separation of 8-aminonaphthalene-1,3,6-trisulfonic acid-labelled neutral and sialylated N-linked complex oligosaccharides by capillary electrophoresis

Antje Klockow<sup>a,b</sup>, Renato Amadò<sup>b</sup>, H. Michael Widmer<sup>a</sup>, Aran Paulus<sup>a,\*</sup>

<sup>a</sup>*Ciba, Corporate Analytical Research, CH-4002 Basle, Switzerland*

<sup>b</sup>*Swiss Federal Institute of Technology (ETH Zürich), Institute of Food Science, CH-8092 Zürich, Switzerland*

### Abstract

Complex oligosaccharides, both neutral and sialylated, were derivatized with 8-aminonaphthalene-1,3,6-trisulfonic acid (ANTS) and separated by capillary electrophoresis. The derivatization reaction was carried out in a total reaction volume of 2  $\mu$ l. The separated peaks were detected by laser-induced fluorescence detection using the 325-nm line of a He–Cd laser. Concentration and mass detection limits of  $5 \cdot 10^{-8}$  M and 500 amol, respectively, could be achieved. The limiting step for higher sensitivity is not the detector performance, however, but the chemistry with a derivatization limit of  $2.5 \cdot 10^{-6}$  M. Two labelling protocols were established, one with overnight reaction at 40°C and the other with a 2.5-h derivatization time at 80°C. Neutral oligosaccharides could be labelled with either protocol. However, sialylated oligosaccharides hydrolysed when labelled at 80°C. Low nanomole and picomole amounts of oligomannose-type and complex-type oligosaccharide mixtures were derivatized and separated in less than 8 min with excellent resolution using a phosphate background electrolyte at pH 2.5. The linear relationship between the electrophoretic mobility and the charge-to-mass ratios of the ANTS conjugates was used for peak assignment. Further, the influence of the three-dimensional structure of the complex oligosaccharides on their migration behaviour is discussed. The suitability of the ANTS derivatization and the subsequent separation for the analysis of complex oligosaccharide patterns is demonstrated with oligosaccharide libraries derived from ovalbumin and bovine fetuin. For peak assignment the patterns are compared with those of the oligomannose and the complex-type oligosaccharide mixtures. The separation efficiency of 120 000 theoretical plates and analysis times of less than 10 min are superior to those with state-of-the-art chromatographic methods and other capillary electrophoresis separation methods. A migration time difference of 0.06 min was found to be sufficient for the baseline separation of complex oligosaccharides.

### 1. Introduction

Complex oligosaccharides as found in the glycan moieties of glycoproteins typically consist of 8–14 monosaccharide units. Composed of only seven different glycosidic monomers, they

are characterized by a wide variety of different intermolecular glycosidic bonds, resulting in an enormous multitude of possible structures. In glycoproteins, complex carbohydrates can be linked to the polypeptide chain via an O-glycosidic bond to the hydroxyl group of a serine or threonine residue or via an N-glycosidic bond formed with the side-chain of an asparagine

\* Corresponding author.

residue. Complex carbohydrates are involved in a number of biological recognition processes such as cell–cell interactions, cell development, cell differentiation, hormone–receptor and antigen–antibody interactions [1,2]. In addition, glycosylation increases the proteolytic resistance of proteins. A number of therapeutic proteins are produced by recombinant techniques in mammalian cells. Because these proteins are often expressed with glycan moieties which affect their biological activity, lifetime and specificity, control of correct glycosylation of these drugs is a very important issue [3].

It is generally accepted that the specificity and activity of glycoproteins are determined not only by the amino acid sequence of the protein part but also by the composition and structure of its glycan moieties. In contrast to proteins and nucleic acids, where the molecular alphabet has been deciphered, the “sugar language” of complex carbohydrates remains a challenging scientific problem because of the considerable structural diversity of complex carbohydrates.

The limited amount of sample released from purified glycoproteins adds to the analytical demand for highly sensitive and selective methods. In general, amino acid sequence information can be obtained with 10 pmol of purified protein. This also limits the amount of oligosaccharides available for further analysis. If all carbohydrate can be completely derivatized in 10  $\mu$ l, the concentration detection limit of the analytical method has to be lower than  $10^{-6}$  M while still allowing the selective separation of closely related solutes.

Several electrophoretic and chromatographic techniques have been used for the determination of mono- and oligosaccharide mixtures, with high-performance anion-exchange chromatography combined with pulsed amperometric detection (HPAEC–PAD) as the state-of-the-art method. However, with a mass detection limit of ca. 10 pmol [4], corresponding to a concentration detection limit of  $10^{-6}$  M, HPAEC–PAD is short of the sensitivity necessary for complex carbohydrate analysis in bioresearch applications.

Capillary electrophoresis (CE) evolved as a promising alternative in carbohydrate analysis

with respect to fast and highly efficient separations. Since neutral carbohydrates lack both charge and chromophores for CE analysis, several strategies have been discussed for the on-column detection of carbohydrates after CE separation. The on-column complexation with borate results in a 2–20-fold increase in the UV signal at 195 nm, thus allowing detection at a millimolar level [5]. With indirect photometric detection using sorbic acid, detection limits in the higher micromolar ( $10^{-4}$ – $10^{-5}$  M) range could be achieved [6–8]. Amperometric detection has recently been reported to allow selective detection at the  $10^{-6}$  M level for reducing and non-reducing carbohydrates [9]. However, similarly to refractive index detection in CE, the applicability of which to carbohydrate analysis has been demonstrated [10], amperometric detection is not yet commercially available for CE and consequently is limited in its use for most biochemical laboratories.

Precolumn derivatization therefore seems to be the most promising approach for the sensitive detection of carbohydrates. Several labelling procedures for carbohydrates for sensitive UV and/or fluorescence detection have been described in the literature. The most frequently used procedure for reducing carbohydrates consists in their reductive amination with a chromophore or fluorophore containing a primary amino group, such as 2-aminopyridine [11], *p*-amino- or ethyl-*p*-aminobenzoic acid [12,13] or 4-aminobenzonitrile [14]. A base-catalysed condensation for reducing carbohydrates with the active hydrogens of 3-methyl-1-phenyl-2-pyrazolin-5-one (MPP) was developed by Honda et al. [15]. UV detection of 2-aminopyridine-, *p*-aminobenzoic acid- or MPP-labelled carbohydrates resulted in detection limits of  $(4–8) \cdot 10^{-6}$  M [15,16]. UV detection limits reported to date are therefore insufficient to detect labelled glycoprotein-derived oligosaccharides even if purification, release and labelling can be performed on a theoretical level.

The lowest concentration detection limit of  $10^{-9}$  M was reported using laser-induced fluorescence (LIF) detection of 3-(4-carboxybenzoyl)-2-quinolinecarboxyaldehyde (CBQCA) carbohy-

drate derivatives [17]. CBOCA reacts with aminoglycans, which are formed by reductive amination of carbohydrates with ammonia. This two-step labelling procedure is also hampered by a narrow range of molar excess of label to obtain the maximum derivatization yield [18]. However, LIF detection schemes provide the hope of achieving the submicromolar detection limits necessary for glycoprotein-derived oligosaccharides when suitable labels and optimized labelling conditions can be worked out.

Separation in CE relies on charge and size differences. As the majority of carbohydrates lack readily ionizable groups, their electrophoretic separation is difficult. An approach frequently used to overcome this difficulty is the complexation of the carbohydrate with borate at high pH, forming anionic species [5]. Under these conditions, a strong electroosmotic flow (EOF), generated at the negatively charged inner capillary wall, drives all solutes from the cathodic injection side towards the detector. Labels carrying pH-independent charges would allow more flexibility in the choice of electrolyte composition as for pH and additives.

As positive charges tend to adsorb on the negatively charged capillary wall of an unmodified fused-silica capillary, a negatively charged label is preferred. Labelling strategies involving derivatives of aromatic sulfonic acids such as 7-aminonaphthalene-1,3-disulfonic acid (ANDS) and 8-aminonaphthalene-1,3,6-trisulfonic acid (ANTS) seem to be very promising, since the corresponding carbohydrates derivatives are highly charged even at low pH, which is important with respect to the optimization of resolution.

The resolution of two compounds in any separation system depends on the efficiency, given by the number of theoretical plates and the selectivity of the solutes measured by the difference in their migration velocity [19]. In CE, migration velocity is the vectorial sum of electroosmotic ( $\mu_{eo}$ ) and electrophoretic ( $\mu_{ep}$ ) mobility. With an increase in electroosmotic flow (EOF) under otherwise identical conditions, the resolution of two solutes decreases because the difference in migration times decreases. Op-

timum resolution can be achieved by balancing the EOF against the electrophoretic migration velocity of the solutes. At a highly acidic pH, the electrophoretic migration velocity of the negatively charged ANDS- or ANTS-labelled carbohydrates is larger than the small EOF in fused-silica capillaries. This allows fast and high-resolution separations.

The derivatization of reducing carbohydrates with ANTS was first described by Jackson [20] for use in slab gel electrophoresis. Applications of ANTS [21–23] and ANDS [24] labelling procedures to mono- and oligosaccharides with subsequent CE separations were published recently.

In this work, the ANTS labelling scheme was applied to the determination of glycoprotein-derived complex oligosaccharides. Mass and concentration limits with He–Cd laser LIF detection were investigated, especially with respect to the minimum sample amount that can be derivatized and detected. Rapid and high-resolution CE separations of oligomannose- and complex-type oligosaccharide mixtures are demonstrated. The influence of charge and mass of the ANTS-labelled oligosaccharides on their elution order is discussed. Finally, oligosaccharide libraries, released from ovalbumin and fetuin, were ANTS labelled and separated by CE. A complete interpretation of the complex library pattern was not possible with the available data; however, by comparison of the migration data with those for purified standard complex oligosaccharides and by establishing mobility versus charge-to-mass ratio relationships, tentative peak assignments were made.

## 2. Experimental

### 2.1. Chemicals

All complex oligosaccharide standards and glycoprotein oligosaccharide libraries were supplied by Oxford Glyco Systems (Abingdon, UK). The derivatization reaction was carried out with ANTS, purchased from Molecular Probes (Eugene, OR, USA), sodium cyanoborohydride

(NaCNBH<sub>3</sub>) and acetic acid from Sigma (Buchs, Switzerland) and dimethyl sulfoxide (DMSO) from Fluka (Buchs, Switzerland). Sodium dihydrogenphosphate (NaH<sub>2</sub>PO<sub>4</sub>) and the sodium hydroxide for the background electrolyte were supplied by Merck (Darmstadt, Germany) and Fluka.

## 2.2. Instrumentation

CE separations were performed on a P/ACE 2100 system (Beckman, Fullerton, CA, USA), equipped with an LIF module. The original Ar ion laser was replaced with a He–Cd laser (Omnichrome, Chino, CA, USA), which was connected to the P/ACE instrument detector via a UV-transmissible optical fibre (Laaber Faser-optik, Munich, Germany). The ANTS-labelled carbohydrates were excited with the 325-nm line of the He–Cd laser with ca. 2 mW. Collimated fluorescence radiation was passed through a 520-nm bandpass filter.

## 2.3. Electrophoresis

All separations were carried out in 50  $\mu\text{m}$  I.D. capillaries with an overall length of 27 cm and an effective separation length of 20 cm with 50 mM phosphate background electrolyte titrated to pH 2.5 and 2 M hydrochloric acid. Since under these conditions the EOF is smaller ( $1.25 \cdot 10^{-5} \text{ cm}^2/\text{V}\cdot\text{s}$ ) than the electrophoretic mobility of triply negatively charged carbohydrates [ $(12\text{--}19) \cdot 10^{-5} \text{ cm}^2/\text{V}\cdot\text{s}$ ], the power supply polarity was reversed with the anodic side at the detector. Between runs the capillary was flushed with 100 mM sodium hydroxide and background electrolyte for 2 min each.

Throughout all experiments, the capillaries were thermostated at 25°C. The injections at the cathodic end of the capillary were performed hydrodynamically. An injection pressure of 35 mbar and injection times of 2, 3 and 6 s resulted in injection volumes of 4, 6 and 12 nl, respectively.

## 2.4. Derivatization procedure

The optimization of the derivatization reaction was described in a previous paper [21]. For the

carbohydrates analysed in this study, two different sets of conditions were used, one for overnight reaction at low temperature (standard conditions) and one at elevated temperature (fast conditions). In both sets, 5  $\mu\text{g}$  of complex oligosaccharide, corresponding to ca. 3 nmol, or 50  $\mu\text{g}$  of a glycoprotein oligosaccharide library were dissolved in 1  $\mu\text{l}$  of a 0.15 M ANTS solution in acetic acid–water (3:17 v/v). In the standard procedure with very mild derivatization conditions, 1  $\mu\text{l}$  of a 1 M NaCNBH<sub>3</sub> solution in DMSO was added to the ANTS–carbohydrate solution. After vortex mixing, the reaction mixture was incubated in a heating block at 40°C for 15 h. When a faster derivatization time was required, the ANTS–carbohydrate solution was heated to 80°C. After 30 min of preincubation, the NaCNBH<sub>3</sub> was added. The derivatization was complete within 2.5 h. Prior to injection, the samples were diluted 100–200-fold.

## 2.5. N-Linked oligosaccharides

The complex oligosaccharides used in these experiments were exclusively of the N-linked type. All N-linked oligosaccharides share the same pentasaccharide core structure M<sub>3</sub>GN<sub>2</sub> (see Table 1), which attaches the oligosaccharides to the asparagine residue of the polypeptide. This core element is extended through the attachment of a number of monosaccharides in different branching patterns. Based on compositional similarities, these carbohydrates are classified as oligomannose- or high-mannose-, hybrid- and complex-type structures. In oligomannose-type oligosaccharides, only mannose is attached to the pentasaccharide core. In the complex-type structures, the core is extended by the addition of various monosaccharides such as N-acetylglucosamine, galactose or sialic acid, but not mannose. The hybrid-type oligosaccharides contain mannose residues in the  $\alpha$ -(1,6) branch of the core element and residues other than mannose in the  $\alpha$ -(1,3) branch.

The oligosaccharides investigated in this study are all of the oligomannose- or complex-type structure (see Table 1). According to the supplier, all carbohydrate samples were released from a defined glycoprotein by hydrazinolysis

Table 1  
N-Linked complex oligosaccharides

Oligomannose type		<p><b>MAN<sub>5</sub>'</b> (<math>M_r = 1235</math>) <i>Oligomannose 5</i></p>
		<p><b>MAN6</b> (<math>M_r = 1398</math>) <i>Oligomannose 6</i></p>
		<p><b>MAN7</b> (<math>M_r = 1560</math>) <i>Oligomannose 7</i></p>
		<p><b>MAN8</b> (<math>M_r = 1398</math>) <i>Oligomannose 8</i></p>
		<p><b>MAN9</b> (<math>M_r = 1398</math>) <i>Oligomannose 9</i></p>
Neutral complex type		<p><b>NA2</b> (<math>M_r = 1642</math>) <i>Asialo-, galactosylated bi-antennary</i></p>
		<p><b>NA2B</b> (<math>M_r = 1845</math>) <i>Asialo-, galactosylated bi-antennary, with bisecting GN</i></p>

(Continued on p. 246)

Table 1 (continued)

	$  \begin{array}{c}  \text{G}\beta\text{1} - 4\text{GN}\beta\text{1} - 2\text{M}\alpha\text{1} \begin{array}{l} \diagdown 6 \\ \diagup 3 \end{array} \\  \text{G}\beta\text{1} - 4\text{GN}\beta\text{1} - 2\text{M}\alpha\text{1} \begin{array}{l} \diagdown 6 \\ \diagup 3 \end{array}  \end{array}  $	$  \begin{array}{c}  \text{F}\alpha\text{1} \\    \\  \text{M}\beta\text{1} - 4\text{GN}\beta\text{1} - 4\text{GN}  \end{array}  $	<b>NA2F</b> ( $M_r = 1788$ ) <i>Asialo-, galactosylated bi-antennary, core-substituted with fucose</i>
	$  \begin{array}{c}  \text{G}\beta\text{1} - 4\text{GN}\beta\text{1} - 2\text{M}\alpha\text{1} \begin{array}{l} \diagdown 6 \\ \diagup 3 \end{array} \\  \text{G}\beta\text{1} - 4\text{GN}\beta\text{1} \begin{array}{l} \diagdown 4 \\ \diagup 2 \end{array} \\  \text{G}\beta\text{1} - 4\text{GN}\beta\text{1} \begin{array}{l} \diagdown 4 \\ \diagup 2 \end{array}  \end{array}  $	$  \begin{array}{c}  \text{M}\beta\text{1} - 4\text{GN}\beta\text{1} - 4\text{GN}  \end{array}  $	<b>NA3</b> ( $M_r = 2005$ ) <i>Asialo-, galactosylated tri-antennary</i>
	$  \begin{array}{c}  \text{G}\beta\text{1} - 4\text{GN}\beta\text{1} \begin{array}{l} \diagdown 6 \\ \diagup 2 \end{array} \\  \text{G}\beta\text{1} - 4\text{GN}\beta\text{1} \begin{array}{l} \diagdown 6 \\ \diagup 2 \end{array} \\  \text{G}\beta\text{1} - 4\text{GN}\beta\text{1} \begin{array}{l} \diagdown 4 \\ \diagup 2 \end{array} \\  \text{G}\beta\text{1} - 4\text{GN}\beta\text{1} \begin{array}{l} \diagdown 4 \\ \diagup 2 \end{array}  \end{array}  $	$  \begin{array}{c}  \text{M}\alpha\text{1} \begin{array}{l} \diagdown 6 \\ \diagup 3 \end{array} \\  \text{M}\beta\text{1} - 4\text{GN}\beta\text{1} - 4\text{GN}  \end{array}  $	<b>NA4</b> ( $M_r = 2373$ ) <i>Asialo-, galactosylated tetra-antennary</i>
	$  \begin{array}{c}  \text{GN}\beta\text{1} \begin{array}{l} \diagdown 6 \\ \diagup 2 \end{array} \\  \text{GN}\beta\text{1} \begin{array}{l} \diagdown 6 \\ \diagup 2 \end{array} \\  \text{GN}\beta\text{1} \begin{array}{l} \diagdown 4 \\ \diagup 2 \end{array} \\  \text{GN}\beta\text{1} \begin{array}{l} \diagdown 4 \\ \diagup 2 \end{array}  \end{array}  $	$  \begin{array}{c}  \text{M}\alpha\text{1} \begin{array}{l} \diagdown 6 \\ \diagup 3 \end{array} \\  \text{M}\beta\text{1} - 4\text{GN}\beta\text{1} - 4\text{GN}  \end{array}  $	<b>NGA4</b> ( $M_r = 1724$ ) <i>Asialo-, agalacto-, tetra-antennary</i>
Sialylated complex type	$  \begin{array}{c}  \text{NAc2} - 3/6\text{G}\beta\text{1} - 4\text{GN}\beta\text{1} - 2\text{M}\alpha\text{1} \begin{array}{l} \diagdown 6 \\ \diagup 3 \end{array} \\  \text{NAc2} - 3/6\text{G}\beta\text{1} - 4\text{GN}\beta\text{1} - 2\text{M}\alpha\text{1} \begin{array}{l} \diagdown 6 \\ \diagup 3 \end{array}  \end{array}  $	$  \begin{array}{c}  \text{M}\beta\text{1} - 4\text{GN}\beta\text{1} - 4\text{GN}  \end{array}  $	<b>A2</b> $M_r = 2224$ <i>Di-sialylated-, galactosylated bi-antennary</i>
	$  \begin{array}{c}  \text{NAc2} - 3/6\text{G}\beta\text{1} - 4\text{GN}\beta\text{1} - 2\text{M}\alpha\text{1} \begin{array}{l} \diagdown 6 \\ \diagup 3 \end{array} \\  \text{NAc2} - 3/6\text{G}\beta\text{1} - 4\text{GN}\beta\text{1} \begin{array}{l} \diagdown 4 \\ \diagup 2 \end{array} \\  \text{NAc2} - 3/6\text{G}\beta\text{1} - 4\text{GN}\beta\text{1} \begin{array}{l} \diagdown 4 \\ \diagup 2 \end{array}  \end{array}  $	$  \begin{array}{c}  \text{M}\beta\text{1} - 4\text{GN}\beta\text{1} - 4\text{GN}  \end{array}  $	<b>A3</b> $M_r = 2881$ <i>Tri-sialylated, galactosylated tri-antennary</i>

NAc = N-acetylneuraminic acid, G = galactose, GN = N-acetyl-glucosamine, M = mannose, F = fucose.

and subsequently purified by various chromatographic procedures [25].

### 3. Results and discussion

The derivatization scheme for complex oligosaccharides is based on the reductive amination of the reducing carbonyl group of the oligosaccharide with the primary amino group of a chromophore or fluorophore. The primary reaction product is a Schiff base, which is subsequently reduced (and stabilized) to a secondary amine by sodium cyanoborohydride (Fig. 1).

#### 3.1. Derivatization sensitivity and minimum sample amount

In a previous study [21], maltose was used as a model carbohydrate to establish optimum label-

#### N-LINKED OLIGOSACCHARIDE DYE

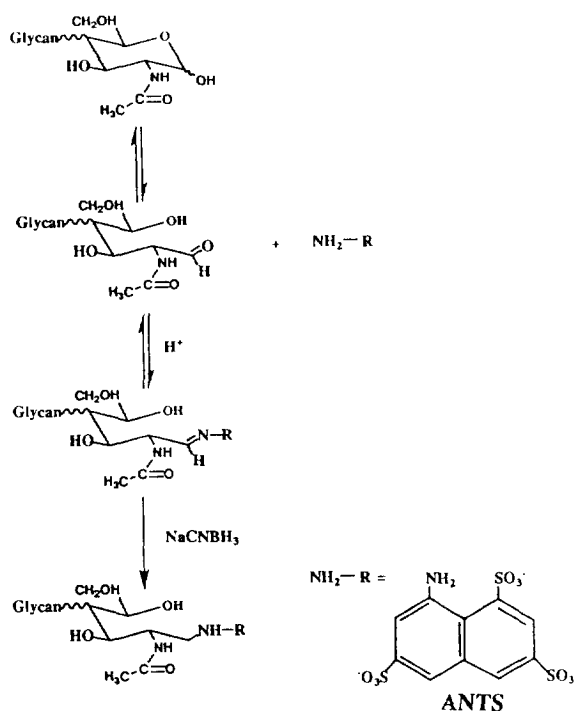


Fig. 1. Reaction scheme for the derivatization of complex oligosaccharides by reductive amination.

ling conditions with respect to derivatization time, temperature and acetic acid concentration. Using volumes as small as  $2 \mu\text{l}$  and low nanomolar amounts of carbohydrate in the derivatization reaction, a concentration detection limit (LOD) of  $5 \cdot 10^{-8} \text{ M}$  could be achieved with LIF detection, using the 325-nm line of a He–Cd laser. This corresponds to a mass detection limit of 500 amol injected, assuming a 10-nl injection volume. Both concentration and mass detection limits were found to be dependent on the molecular mass of the oligosaccharide, since the overall derivatization yield decreases slightly with increasing size of the oligosaccharide. For the present study, the optimum conditions found for maltose were transferred to complex oligosaccharides yielding the same mass and concentration sensitivities.

Mass and concentration detection limits for labelled solutes are in general determined by serial dilutions of derivatization reactions carried out at the milli- or micromolar level for both reactants. However, in a biochemistry laboratory not only the detector performance but also the minimum amount of sample that can be labelled and detected after derivatization is of interest. Therefore, a series of ANTS derivatizations of two complex oligosaccharides, NA2 and NA3 (for structures see Table 1), were carried out. The absolute amounts ranged from 500 to 12 pmol, corresponding to  $1 \mu\text{g}$ –25 ng total carbohydrate. Fig. 2 demonstrates that as little as 25 pmol (50 ng) of NA3 could be detected after ANTS labelling. For the smaller NA2, the minimum amount of 12 pmol (20 ng) was even lower, because the reaction yield is higher with smaller carbohydrates.

Since for the experiment all carbohydrates were in a final volume of  $10 \mu\text{l}$  prior to injection, the concentration of the complex carbohydrate can be calculated to be  $(1.2\text{--}2.5) \cdot 10^{-6} \text{ M}$ . This is what we call the derivatization limit of the ANTS labelling of oligosaccharides. The derivatization limit is of practical importance since it takes detector performance and reaction efficiency into account. The concentration detection limit of  $5 \cdot 10^{-8} \text{ M}$  with the LIF detection system is 1.5 orders of magnitude better than the

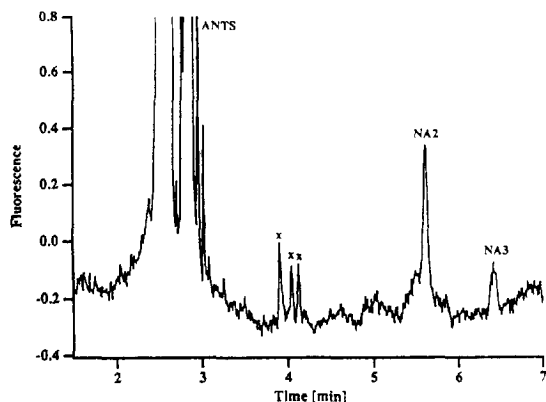


Fig. 2. Derivatization limit for complex oligosaccharides. Derivatization and separation of 25 pmol of NA2 and NA3. CE conditions: electrolyte, 50 mM phosphate (pH 2.5); capillary, 27 cm (20 cm effective length)  $\times$  50  $\mu$ m I.D.; voltage, 10 kV; temperature, 25°C; injection time, 6 s; He–Cd laser with LIF detection: excitation at 325 nm, emission at 520 nm.  $\times$  = Unknown peaks, generated from the ANTS label during derivatization.

lowest carbohydrate concentration of  $1.2 \cdot 10^{-6}$  M that can currently be derivatized with ANTS. This means that the detector potential is not yet fully utilized, because the chemistry is the limiting factor and procedures for labelling at the submicromolar level are not commonly available.

With an injection volume of 10 nl, an absolute amount of 25 fmol per peak is introduced into a capillary. In contrast, the lowest detectable amount of complex carbohydrates reported with slab gel electrophoresis is 5 pmol per band of ANTS conjugate [20].

### 3.2. Sialylated oligosaccharides

Complex oligosaccharides carrying sialic acid residues attached to the end of the antennae, such as A2 or A3 (Table 1), are of special interest, because the degree of sialylation of the glycan moieties is believed to be responsible for the microheterogeneity of glycoproteins [26]. Therefore, a method capable of differentiating complex carbohydrates according to the number of sialic acid residues incorporated would allow at least a first assessment of native microheterogeneity.

Since the  $\alpha$ -(2,3) and  $\alpha$ -(2,6) linkages of the

sialic acids are sensitive to hydrolysis, special attention should be paid during the optimization of the derivatization procedure. Because the reductive amination is acid catalysed, the presence of acetic acid in the reaction mixture was evaluated with respect to the stability of the sialic acid residues during the derivatization of sialylated carbohydrates. In addition, temperature and reaction time were also investigated.

Experiments with neutral oligosaccharides demonstrated their stability under reaction conditions in the presence of 15% acetic acid at 40°C for at least 15 h. To evaluate the influence of the acetic acid on the stability of the sialylated oligosaccharides, an A3 sample was labelled in the presence of 15% acetic acid, whereas in a control experiment acetic acid was omitted. The electropherograms for both A3 samples look almost identical, with one main peak followed by two smaller ones (see Fig. 3a). If sialic acid is hydrolysed during the labelling reaction, one would expect to see also the non-sialylated species. Therefore, the neutral “analogon” of A3, NA3, was labelled under standard conditions. In the acidic buffer medium, the A3 samples with a molecular mass of 3291 migrate faster than the corresponding smaller NA3 with a mass of 2417. The migration times of 5.63 and 5.90 min for A3 and 7.19 min for NA3 (Fig. 3a) clearly demonstrate that additional negative charges from the sialic acid accelerate the migration of the larger A3.

Although the electropherograms obtained after labelling in the presence or absence of acetic acid show identical products, the derivatization yield is vastly different. The A3 sample labelled in the presence of 15% acetic acid resulted in a tenfold larger peak area compared with the control sample without acetic acid. It seems that acetic acid is an important catalyst in the derivatization of reducing carbohydrates by reductive amination. The mechanism of this catalytic effect is not clear as, owing to the dissociation of the sulfonic acid groups of ANTS, the reaction solution has an almost identical pH (pH 1.6 and 1.8, respectively) in the presence or absence of acetic acid. Therefore, acetic acid cannot act as an acidic catalyst as it is completely protonated under these conditions.



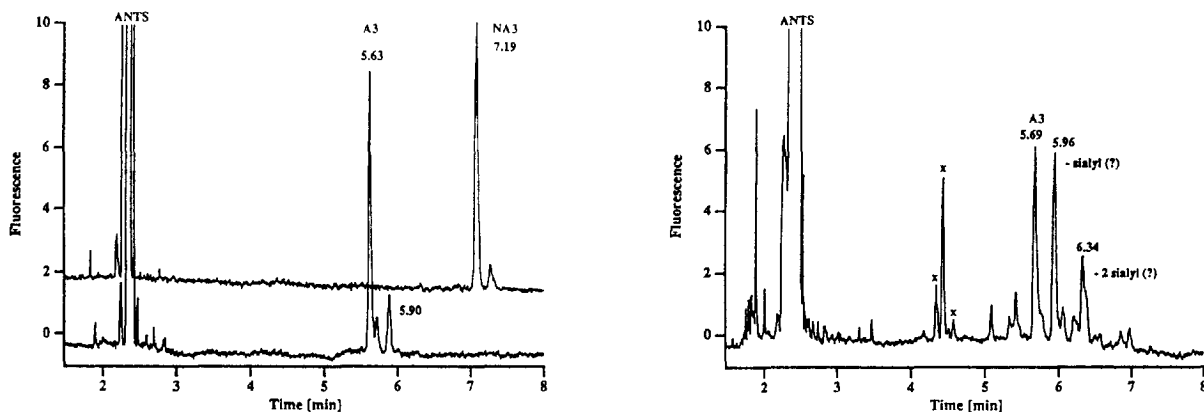


Fig. 3. Electropherogram of (a, left) the neutral triantennary oligosaccharide NA3 and its trisialylated analogon A3 derivatized with ANTS at 40°C for 15 h and (b, right) the sialylated A3 derivatized with ANTS at 80°C for 2.5 h. CE conditions as in Fig. 2, except injection time, 3 s.

Labelling optimization with maltose demonstrated that with an increased temperature of 80°C the reaction time could be reduced to 2.5 h if the cyanoborohydride was added in a second step after 30 min [21]. With neutral complex oligosaccharides no degradation was observed on heating to 80°C. In Fig. 3, A3 was labelled under standard conditions (40°C, 15 h, Fig. 3a) and fast conditions (80°C, 2.5 h, Fig. 3b). A comparison of the two electropherograms reveals sample degradation of the sialylated oligosaccharide at 80°C, since not just one major peak but at least three main peaks can be observed. Most likely these peaks are generated through desialylation of the A3 molecule.

### 3.3. Standard mixtures

An oligomannose-type and a complex-type oligosaccharide mixture were prepared to characterize the separation system. The oligomannoses were derivatized as a mixture, containing MAN5 to MAN9, and as purified samples MAN5, MAN8 and MAN9. The complex-type mixture was made up by mixing the individually labelled oligosaccharides.

#### Oligomannose-type panel

The separation of the five oligomannose-type carbohydrates is shown in Fig. 4. The solutes migrate in order of increasing molecular mass, with the smaller MAN5 eluting first and the

larger MAN9 last. The peak to peak mass difference is 162, equivalent to the mass of one anhydrous mannose residue. All solutes carry the same three negative charges from the ANTS label.

For peak identification, individual oligomannose standards were labelled and injected and their migration times were compared with those of the mixture. In this way, MAN5, MAN8 and MAN9 could be clearly assigned. Given the regular, oligomeric nature of the sample, the two major peaks between MAN5 and MAN8 were assigned to MAN6 and MAN7.

According to electrophoretic theory, an ion or particle migrates in free solution in an electrical field with an electrophoretic mobility,  $\mu_{ep}$ , that is proportional to its electrical charge,  $q$ , and inversely proportional to viscosity,  $\eta$ , and its hydrodynamic radius,  $R$  [27]:

$$\mu_{ep} = q/6\pi\eta R \quad (1)$$

Although Eq. 1 holds true only for small, symmetrical, spherical ions in infinite dilution, it can also be applied to larger solutes. As the hydrodynamic radius is related to the size and molecular mass, the charge-to-mass ratio,  $q/M$ , of a solute should be proportional to its electrophoretic mobility in free solution electrophoresis.

For all complex carbohydrates used in this work, Table 2 lists the molecular masses of the

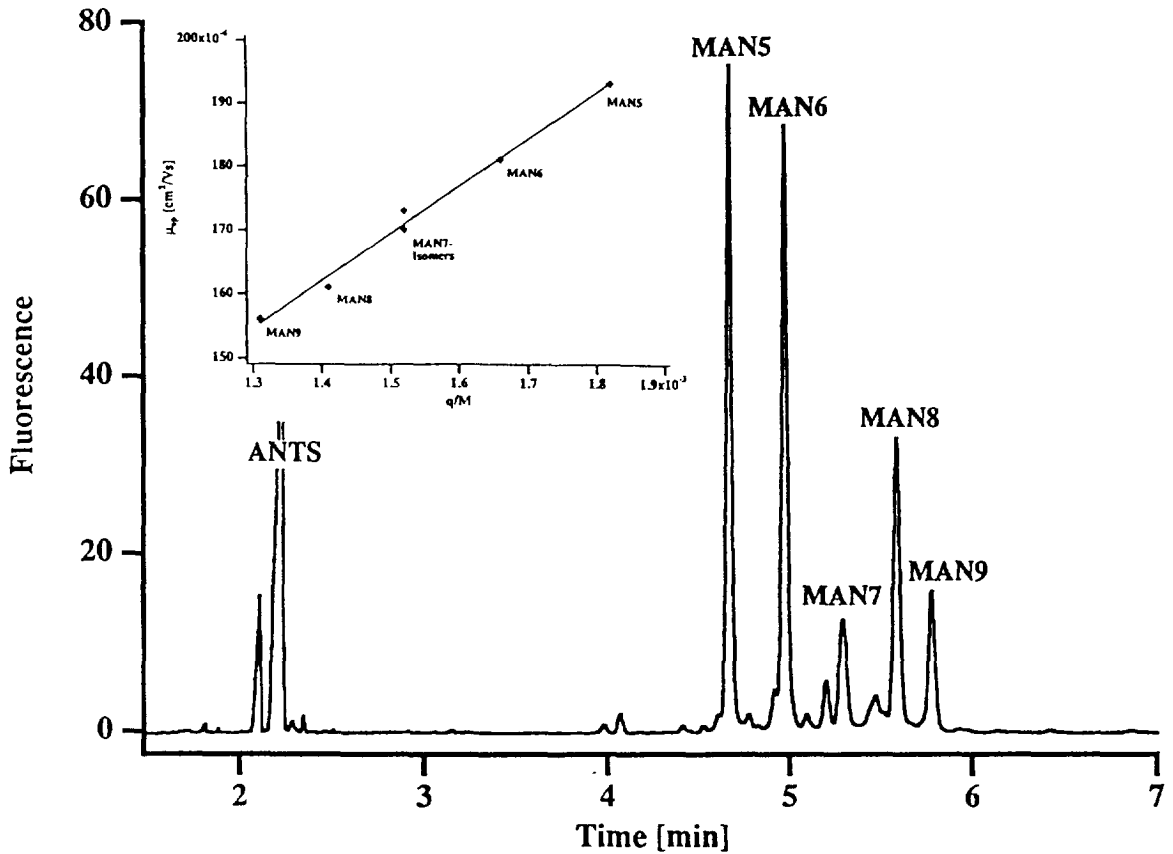


Fig. 4. Separation of ANTS-labelled oligomannose-type oligosaccharides MAN5 to MAN9. CE conditions as in Fig. 2. Sample: 50  $\mu\text{g}$  per 2  $\mu\text{l}$  of derivatized MAN mixture, 250  $\mu\text{g}/\text{ml}$  injected. Inset:  $\mu_{\text{ep}}$  versus  $q/M$  relationship for the MAN5–9 ANTS derivatives:  $y = 5.839 \cdot 10^{-5} + 0.074 \cdot x$ ,  $r = 0.995$ .

Table 2

Electrophoretic mobilities ( $\mu_{\text{ep}}$ ) and charge-to-mass ratios of various neutral and sialylated N-linked oligosaccharides

Oligosaccharide	Mass (g/mol)	+ANTS (g/mol)	Charge	Charge/mass $\times 10^{-3}$	$t_{\text{M}}$ (min)	$\mu_{\text{ep}}$ ( $10^{-5} \text{ cm}^2/\text{V} \cdot \text{s}$ )
MAN5	1235	1645	-3	1.82	4.67	19.3
MAN6	1398	1808	-3	1.66	4.97	18.1
MAN7	1560	1970	-3	1.52	5.20/5.29	17.3/17.0
MAN8	1722	2132	-3	1.41	5.58	16.1
MAN9	1884	2294	-3	1.31	5.78	15.6
NGA4	1724	2134	-3	1.41	5.66	15.9
NA2	1642	2052	-3	1.46	5.77	15.6
NA2B	1845	2255	-3	1.33	5.85	15.4
NA2F	1788	2198	-3	1.36	5.99	15.0
NA3	2005	2415	-3	1.24	6.69	13.7
NA4	2373	2783	-3	1.08	7.31	12.3
A2	2224	2634	-5	1.90	5.10	17.6
A3	2881	3291	-6	1.82	5.41	16.6

pure and ANTS-labelled carbohydrates, the number of charges, assuming  $-3$  for ANTS and  $-1$  for each sialic acid, the charge-to-mass ratio,  $q/M$ , the migration time,  $t_m$ , in the pH 2.5 phosphate background electrolyte and the electrophoretic mobility,  $\mu_{ep}$ . The data for the oligomannose-type carbohydrates including the assumed assignments of MAN6 and MAN7 are plotted as  $\mu_{ep}$  versus  $q/M$  in the inset in Fig. 4 and yield a linear relationship with  $y = 5.839 \cdot 10^{-5} + 0.074x$ ,  $r = 0.995$ . Since all oligomannose-type carbohydrates are neutral, having the same number of three negative charges originating from the ANTS label, their migration order is according to the increasing number of mannose residues. A higher charge-to-mass ratio is therefore equivalent to a lower molecular mass. The linear  $\mu_{ep}$  versus  $q/M$  relationship thus confirms the peak assignment of MAN6 and MAN7. This result compares favourably with a recently published separation without labelling [28].

MAN7 and MAN8 can exist as stereoisomers (see Table 1), as confirmed by the specifications of the supplier through HPAEC–PAD analysis. The additional mannose in MAN7, compared with MAN6, can be attached to one of the three branches. However, only two isomers should be present in the sample, in a ratio of 3:7 [29]. The electropherogram also exhibits two peaks in a 3:7 ratio just where the MAN7 should be, adding more evidence to the assignment. Because of the MAN7 isomers, two dots appear in the  $\mu_{ep}$  versus  $q/M$  curve.

A similar argument could be made for MAN8; however, according to the HPAEC–PAD reference chromatogram, both isomers exist only in a ratio smaller than 1:10, resulting in a main peak with a slight shoulder. Without purified isomers, it seems difficult to assign the small preceding peak of MAN8, which could well be a reaction side-product.

A similar attempt to describe the electrophoretic mobility–molecular size relationship appeared recently. Oefner and Chiesa [30] adapted a model developed by Offord [31] for proteins and peptides, with the electrophoretic mobility being inversely proportional to (molecular mass) $^{-2/3}$ . However, the experimentally deter-

mined mobilities do fit the simple and straightforward relationship described above. Additionally, the more complicated model does not take the charge influence into account, a severe limitation for describing the migration behaviour of sialylated complex carbohydrates.

#### Complex-type panel

Fig. 5 shows the separation of six different neutral bi-, tri- and tetraantennary (NA2, NA2B, NA2F, NA3, NA4, NGA4) and two sialylated (A2, A3) complex-type oligosaccharides in the pH 2.5 phosphate background electrolyte in less than 8 min. The sialylation in A2 and A3 accounts for two and three additional negative charges compared with the neutral analogues NA2 and NA3. The additional charges result in higher charge-to-mass ratios and therefore faster migration, despite the increase in molecular mass. The largest neutral oligosaccharides, NA4, has the longest migration time, 7.31 min.

As discussed for the homologous series of oligomannoses, the principal separation mechanism for this set of complex-type oligosaccharides is the difference in the charge-to-mass ratio. However, the strict linear  $\mu_{ep}$  versus  $q/M$  relationship cannot be applied here. As shown in Table 1, the two complex oligosaccharides, NA2B and NA2F, differ in their composition but not in the number of sugar residues. The bisect-

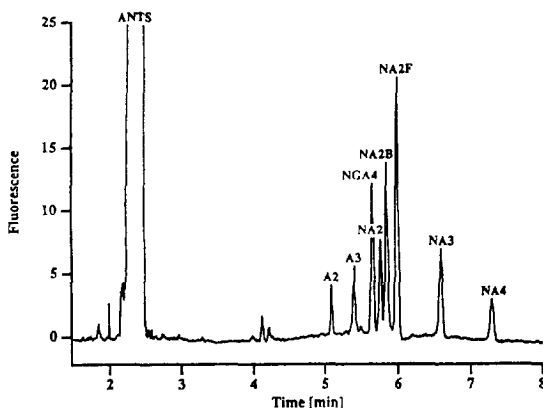


Fig. 5. CE separation of sialylated (A) and neutral (NA) complex-type oligosaccharides. CE conditions as in Fig. 2; oligosaccharide concentration, 3.8–6.1  $\mu M$ .

ing N-acetylglucosamine (GN) in the NA2B is substituted by a fucose (F) residue in the core of the NA2F. This results in a difference in molecular mass of only 57. The corresponding charge-to-mass ratios of  $1.33 \cdot 10^{-3}$  and  $1.36 \cdot 10^{-3}$  for NA2B and NA2F (Table 2), respectively, are not reflected in the separation. Surprisingly, NA2B and NA2F can be well separated, with the larger NA2B migrating in front of NA2F (Fig. 5).

The same is true for the pair NGA4 and NA2, which also contain the same number of sugar residues but differ in composition. NA2 with a charge-to-mass ratio of  $1.46 \cdot 10^{-3}$  migrates more slowly than NGA4, which has a charge-to-mass ratio of only  $1.41 \cdot 10^{-3}$ . On the other hand carbohydrates with a larger mass difference, such as NA2 and NA2B ( $\Delta M = 203$ ), show less resolution than the NA2B–NA2F and the NGA4–NA2 pairs. These two examples demonstrate that the migration behaviour of these complex carbohydrates is affected not only by their charge-to-mass ratio.

It can be assumed that the distinct three-dimensional structure, determined by the steric position of the sialic acids, the glycosidic linkages, the  $\alpha/\beta$  anomerity and the variety of branching, causes a deviation from a simple  $\mu_{ep}$  versus  $q/M$  relationship, which assumes spherical solutes without preferential arrangement in the electrical field. The assumed influence of the three-dimensional structure brings additional selectivity to the separation. The high resolution is a result of a high separation power of at least 120 000 theoretical plates, and the selectivity provided mainly by a  $\mu_{ep}$  versus  $q/M$  dependence, which is applicable only to a series of

homologous compounds, mediated by assumed stereochemical effects. Therefore, even small differences in molecular mass can be sufficient to obtain baseline or close to baseline resolution for the separation of complex oligosaccharides in a very simple separation system.

#### Trisialylated oligosaccharide (A3)

The linear  $\mu_{ep}$  versus  $q/M$  relationship can also be used to explore if the three peaks generated during labelling of A3 at elevated temperature could possibly result from a desialylation process (Fig. 3b). The plot of  $\mu_{ep}$  versus  $q/M$  (calculated values in Table 3) shows a similar linear dependence as demonstrated for the oligomannose-type carbohydrates. The migration times of A3 and NA3 in this data set are not identical with those in Table 2, because of a slight change in EOF over several weeks. However, within one set of experiments, all data are consistent. The corresponding linear equation ( $y = 5.618 \cdot 10^{-5} + 0.0566x$ ) has a high correlation coefficient  $r$  of 0.994. Therefore, the three peaks in Fig. 3b at 5.69, 5.96 and 6.34 min can be assigned to A3 with three, two and one sialic acid, respectively. Complete desialylation of A3 does not occur under the reaction conditions, as no peak is present at the migration time of NA3 (7.20 min), which represents the asialo form of A3. The migration time of NA3 could be predicted with the values for the tri-, bi- and monosialylated species and verified by an independent experiment.

The  $\mu_{ep}$  versus  $q/M$  dependence also allows the assignment of one of the additional peaks that shows up in the separation of A3 (Fig. 3a). By comparing the migration time of the smaller

Table 3  
Electrophoretic mobilities ( $\mu_{ep}$ ) and charge-to-mass ratios of various neutral and sialylated N-linked oligosaccharides

Oligosaccharide	Mass (g/mol)	+ANTS (g/mol)	Charge	Charge/mass $\times 10^{-3}$	$t_M$ (min)	$\mu_{ep}$ ( $10^{-5} \text{ cm}^2/\text{V}\cdot\text{s}$ )
A3	2881	3291	-6	1.82	5.69	15.8
-1 sialyl	2589	2999	-5	1.67	5.96	15.1
-2 sialyl	2297	2707	-4	1.48	6.34	14.2
-3 sialyl (NA3)	2005	2415	-3	1.24	7.20	12.5

peak with the  $\mu_{ep}$  values in Table 2, the signal at 5.90 min can be assigned to the A3 with only two sialic acid residues. That means that the original A3 sample is slightly degraded either during the derivatization or already during the isolation and purification process. Another batch of A3 showed the same pattern after derivatization.

### 3.4. Oligosaccharide libraries

After optimizing the derivatization conditions for neutral and charged oligosaccharide standards, the labelling procedure was applied to oligosaccharide libraries generated from two different glycoproteins, ovalbumin and fetuin. A 50- $\mu\text{g}$  amount of each library was used and labelled under standard conditions to avoid possible degradation. The fetuin sample, which contains a considerable number of highly charged complex carbohydrates, was labelled without acetic acid. After the derivatization, the reaction volume was made up to 20  $\mu\text{l}$  prior to injection.

#### Ovalbumin oligosaccharide library

Ovalbumin, found in hen egg white, is a glycoprotein with a molecular mass of 43 000, containing two possible N-glycosylation sites. Glycosylation accounts for only 3.5% of its mass [32]. The nine oligosaccharides structurally identified belong to either the oligomannose- or hybrid-type structures. Both types are present in ovalbumin in a ratio of ca. 1:1 [33].

Fig. 6a shows the separation of the ANTS-labelled ovalbumin-derived oligosaccharides. In less than 6.5 min, ten peaks could be clearly distinguished. As ovalbumin contains a considerable amount of oligomannose-type oligosaccharides, its carbohydrate pattern was matched with the oligomannose reference pattern (Fig. 6b).

An overlay of the two traces revealed that several peaks with identical migration times are found in the reference and the glycoprotein-derived trace. This could be further confirmed by co-injecting the ovalbumin library and the oligomannose panel. For the co-injection, the two samples were injected one after the other for

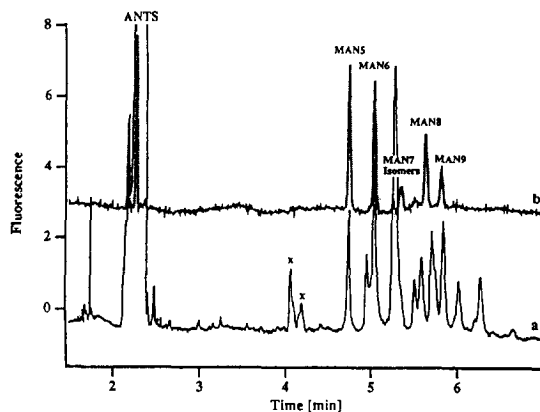


Fig. 6. Comparison of the ovalbumin oligosaccharide pattern (a) with the oligomannose type reference panel (b). CE conditions as in Fig. 2.

2 s. The migration times of double injected samples were independent of the injection order, confirming that co-injection does not bias against the first injected sample. The combined injection volume of  $2 \times 4$  nl corresponds to less than 0.4% of the total capillary volume.

Co-injection of ovalbumin-derived oligosaccharides and the oligomannose-type panel resulted in a co-migration of three of the first four signals of the ovalbumin-derived oligosaccharides with MAN5, MAN6 and MAN7 (Fig. 7). The unambiguous identification of MAN7 in the

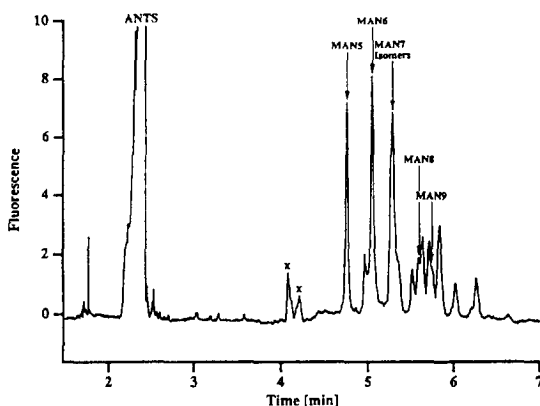


Fig. 7. Co-injection of oligomannose-type reference panel and the ovalbumin oligosaccharide library. CE conditions as in Fig. 2, except injection time, 2 s for each sample.

ovalbumin-derived pattern is not possible, since the concentration of MAN7 in the reference mixture is fairly low compared with the ovalbumin; however, the presence of MAN5 and MAN6 in the ovalbumin library can be ascertained. MAN8 produced a double peak at 5.64 min and migration of MAN9 increased the slight shoulder of an ovalbumin peak at 5.72 min, indicating that these two oligomannoses are not present in the ovalbumin oligosaccharide library. The other peaks in the ovalbumin library can be attributed to the hybrid-type oligosaccharides with eight to eleven carbohydrate residues [34]. A more detailed assignment of the peaks to distinct structures was not possible, since the corresponding oligosaccharide standards were not available.

Honda et al. [35] reported that the capillary electrophoretic separation of the ovalbumin oligosaccharide pool could resolve only five peaks in an acidic phosphate electrolyte [35]. The separation of aminopyridine-labelled carbohydrates is also based primarily on size differences. However, some of the oligomannose- and the hybrid-type oligosaccharides most likely contain the same number of monomers with only small differences in their total molecular masses. The five peaks represent five size classes defined by the number of carbohydrate residues. It is interesting that the ANTS separation system presented here has dramatically improved the resolving power and is able to distinguish clearly ten peaks.

The resolution,  $R_s$ , of two peaks is given by the following equation [19]:

$$R_s = \frac{1}{4} \sqrt{N} \cdot \frac{\Delta u}{\bar{u}} \quad (2)$$

where  $N$  = number of theoretical plates,  $\Delta u$  = difference in migration velocity of two solutes and  $\bar{u}$  = average migration velocity. The minimum difference in migration velocity of two solutes can be calculated by rearrangement:

$$\Delta u = 4R_s \cdot \frac{\bar{u}}{\sqrt{N}} \quad (3)$$

As the migration velocity  $u$  is related to the effective separation length  $l$  with migration time  $t$ , the migration velocity and migration time are inversely proportional at a constant separation length. With a minimum number of theoretical plates of 120 000 and an average migration time of 5.5–6.5 min, baseline resolution ( $R_s = 1$ ) is achieved with a difference in migration time of at least 0.06–0.08 min. This allows very small differences in solute mobility to be sufficient for separation. The first three oligomannose components of the ovalbumin differ by 0.3 min, allowing an easy separation. The other peaks attributed to the hybrid-type carbohydrates are separated with a resolution between 1.5 and 5. Only two shoulders on the MAN7 peak and MAN9 peak indicate that this separation system is not sufficient to resolve the ovalbumin sample completely into all its individual components.

#### *Bovine fetuin oligosaccharide library*

Bovine fetuin, the major glycoprotein in fetal calf serum, represents a highly glycosylated protein, containing O- and N-linked glycan moieties [36]. Bovine fetuin is known to contain a considerable amount of charged oligosaccharides. Among the N-linked glycans, six classes of complex carbohydrates can be distinguished in fetuin corresponding to zero, one, two, three, four and five sialic acid residues in the molecule. The major species are the di-, tri- and tetra-sialylated oligosaccharides, most of them with a triantennary structure [37]. Biantennary structures have also been identified [34].

The separation of the ANTS-labelled oligosaccharide library of bovine fetuin is shown in Fig. 8. The electropherogram can be roughly divided into two parts. The first part is distinguished by very sharp but smaller peaks (2.8–4 min). The second part contains broader, but higher peaks (5–6.7 min). The fetuin library, prepared by hydrazinolysis, contains both N- and O-linked carbohydrate structures. Because O-linked reference carbohydrates were not commercially available, the oligosaccharide pattern was only compared with the N-linked carbohy-

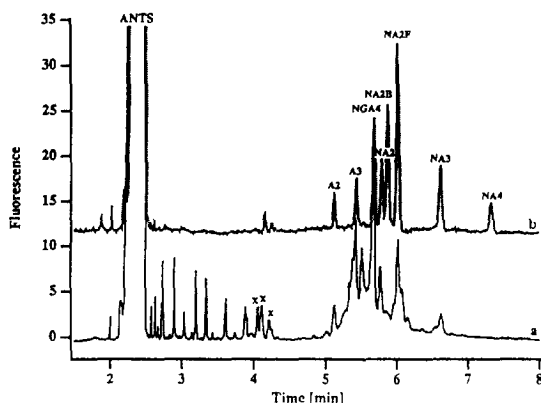


Fig. 8. Comparison of the fetuin oligosaccharide library (a) with the complex-type reference panel, including charged (A) and uncharged (NA) oligosaccharides (b). CE conditions as in Fig. 2.

drates of the complex reference panel. There is no match in the first part of the electropherogram, but the second part shows identical migration times in both electropherograms. A close inspection reveals the co-migration of six fetuin oligosaccharides with the A2, A3, NGA4, NA2, NA2F and NA3 reference oligosaccharides. This could also be confirmed by co-injection of the fetuin and the complex-type oligosaccharide mixture, similarly to the procedure described for ovalbumin.

Fetuin is known to contain the two neutral oligosaccharides, NA2 and NA3 [34], next to the A3 and its various isomeric forms, differing in the position of the sialic acid or the galactose linkages [37]. The two shoulders on the A3 peak in Fig. 8a could possibly be attributed to these isomeric forms.

The peaks in the fetuin panel having the same migration times as NGA4 and NA2F in the complex reference panel could possibly also originate from mono- and disialylated A3. The  $\mu_{ep}$  versus  $q/M$  curve would predict the same migration times. Therefore, a peak assignment is only tentative with the available data. Owing to the complexity of oligosaccharide structures, data from complementary methods will be neces-

sary for complete structural elucidation of oligosaccharide libraries.

#### 4. Conclusions

The ANTS labelling procedure was optimized to allow the electrophoretic separation and detection of both neutral and charged (sialylated) N-linked oligosaccharides under the same conditions. Whereas the neutral oligosaccharides proved to be stable under the conditions for standard and fast derivatization, sialylated oligosaccharides should be handled with care, especially with respect to temperature and acetic acid concentrations during the labelling reaction. Concentration detection limits of  $5 \cdot 10^{-8} M$  can be achieved with LIF detection using the 325-nm line of a He-Cd laser. The derivatization detection limit is of the order of a few micromolar, corresponding to absolute amounts of 10–20 pmol of complex oligosaccharide to be analysed. This is sufficient to work with glycoprotein-derived oligosaccharides.

Further improvements in the detection limit for complex oligosaccharides are not restricted by the detector performance, which is at least 1.5 orders of magnitude better than the derivatization limit. The limiting factor is the chemistry of the labelling reaction. New micromethods have to be developed to work on a microlitre scale, preferably with 1–5  $\mu l$ . The greatest challenge, however, will be to guarantee a quantitative reaction at the dilute concentrations of both solute and label. The mass and concentration detection limits have been pushed to levels unthinkable a few years ago, yet the chemistry to utilize this detection performance has not kept up.

With the current labelling, separation and detection methods, oligosaccharide libraries of various glycoproteins can be analysed, allowing a rapid screening of glycan patterns. With the high separation efficiency for ANTS conjugates and the influence of the molecular structure of the labelled oligosaccharides on their migration, excellent resolution can be achieved. This meth-

od is suitable as a quality control tool to assess the glycosylation of recombinant glycoproteins by comparison with reference libraries.

Peak identification in a separation technique relies on the availability of purified and characterized reference standards. The number of complex oligosaccharides commercially available is still small, but growing. New analytical methods such as that presented here will help to characterize samples purified by chromatographic methods. With a wider selection of complex oligosaccharides, available peak assignment will be facilitated. To compare migration times from run to run better, internal standards might be necessary to eliminate variations introduced by a changing EOF [38].

As the database grows, the interpretation of known and at present unknown oligosaccharide libraries will be possible. A better understanding of unexpected selectivity, presumably introduced by the distinct three-dimensional structure, will also help in an accurate peak assignment and in the correct prediction of migration order. However, as the shoulders in the bovine fetuin library pattern indicate, even the unprecedented selectivity of the current separation system might not be sufficient to resolve all complex oligosaccharides present in a glycan library because the structural variety might be too large.

ANTS derivatization combined with LIF detection has been demonstrated to be suitable as a screening method for the glycosylation pattern of glycoproteins. If the identification of single complex oligosaccharides in mixtures of released glycans can be further advanced, CE with its advantages in speed and resolution could become an effective and valuable tool in the structural elucidation of glycoproteins.

### Acknowledgements

The authors thank Drs. Ernst Gassmann and Beat Krattiger for valuable help with interfacing the He–Cd laser with the P/ACE system. Earlier versions of the manuscript were critically read and commented upon by Drs. Len Cummins (Isis Pharmaceuticals) and Gerard Bruin (Ciba).

### References

- [1] H. Schachter, *Trends Glycosci. Glycotechnol.*, 4 (1992) 241.
- [2] J.M. Paulson, *Trends Biochem. Sci.*, 14 (1989) 272.
- [3] M.W. Spellman, *Anal. Chem.*, 62 (1990) 1714.
- [4] M.R. Hardy and R.R. Townsend, *Proc. Natl. Acad. Sci. U.S.A.*, 85 (1988) 3289.
- [5] S. Hofstetter-Kuhn, A. Paulus, E. Gassmann and H.M. Widmer, *Anal. Chem.*, 63 (1991) 1541.
- [6] A. Klockow, A. Paulus, V. Figueiredo, R. Amadò and H.M. Widmer, *J. Chromatogr.*, 680 (1994) 187.
- [7] A.E. Vorndran, P.J. Oefner, H. Scherz and G.K. Bonn, *Chromatographia*, 33 (1992) 163.
- [8] T.W. Garner and E.S. Yeung, *J. Chromatogr.*, 515 (1990) 639.
- [9] L.A. Colon, R. Dadoo and R.N. Zare, *Anal. Chem.*, 65 (1993) 476.
- [10] A.E. Bruno, B. Krattiger, F. Mayestre and H.M. Widmer, *Anal. Chem.*, 63 (1991) 2689.
- [11] S. Honda, S. Iwase, A. Makino and S. Fujiwara, *Anal. Biochem.*, 176 (1989) 72.
- [12] E. Grill, C. Huber, P.J. Oefner, A.E. Vorndran and G.K. Bonn, *Electrophoresis*, 14 (1993) 1004.
- [13] A.E. Vorndran, E. Grill, C. Huber, P.J. Oefner and G.K. Bonn, *Chromatographia*, 34 (1992) 109.
- [14] H. Schwaiger, P.J. Oefner, C. Huber, E. Grill and G.K. Bonn, *Electrophoresis*, 15 (1994) 941.
- [15] S. Honda, S. Suzuki, A. Nase, K. Yamamoto and K. Kakehi, *Carbohydr. Res.*, 215 (1991) 193.
- [16] P.J. Oefner, A.E. Vorndran, E. Grill, C. Huber and G.K. Bonn, *Chromatographia*, 34 (1992) 308.
- [17] J. Liu, O. Shiota, W. Donald and M. Novotny, *Proc. Natl. Acad. Sci. U.S.A.*, 88 (1991) 2302.
- [18] P.J. Oefner, C. Chiesa, G. Bonn and C. Horváth, *J. Capillary Electrophoresis*, 1 (1994) 5.
- [19] J.C. Giddings, *Sep. Sci.*, 4 (1969) 181.
- [20] P. Jackson, *Biochem. J.*, 270 (1990) 705.
- [21] A. Klockow, H.M. Widmer, R. Amadò and A. Paulus, *Fresenius' J. Anal. Chem.*, 350 (1994) 415.
- [22] C. Chiesa and C. Horváth, *J. Chromatogr.*, 66 (1993) 1134.
- [23] M. Stefanson and M. Novotny, *Anal. Chem.*, 66 (1994) 1134.
- [24] K.-B. Lee, S.-Y. Kim and R.L. Linhardt, *Electrophoresis*, 12 (1991) 636.
- [25] *Tools for Glycobiology*, Oxford Glyco Systems, Abingdon.
- [26] A.D. Tran, S. Park, P. Lisi, O.T. Huynh, R.R. Ryall and P.A. Lane, *J. Chromatogr.*, 542 (1991) 459.
- [27] P.D. Grossman, J.C. Colburn and H.H. Lauer, *Anal. Biochem.*, 179 (1989) 28.
- [28] D.E. Hughes, *J. Chromatogr.*, 657 (1994) 315.
- [29] Technical Note, Reference Panel Oligomannose-Type, Cat. No. RP-2500, Oxford Glyco Systems, Abingdon.
- [30] P.J. Oefner and C. Chiesa, *Glycobiology*, 4 (1994) 397.



- [31] R.E. Offord, *Nature*, 211 (1966) 591.
- [32] N. Tomiya, J. Awaya, M. Kurono, S. Endo, Y. Arata and N. Takahasi, *Anal. Biochem.*, 171 (1988) 73.
- [33] J.P. Landers, R.P. Oda, B.J. Madden and T.C. Spelsberg, *Anal. Biochem.*, 205 (1992) 115.
- [34] S. Suzuki, K. Kakehi and S. Honda, *Anal. Biochem.*, 205 (1992) 227.
- [35] S. Honda, A. Makino, S. Suzuki and K. Kakehi, *Anal. Biochem.*, 191 (1990) 228.
- [36] B. Bendiak, M. Harris-Brandts, S.W. Michnik, J.P. Carver and D.A. Cumming, *Biochem.*, 28 (1989) 6491.
- [37] R.R. Townsend, M.R. Hardy, D.A. Cumming, J.P. Carver and B. Bendiak, *Anal. Biochem.*, 182 (1989) 1.
- [38] P. Hermentin, R. Doenges, R. Witzel, C.H. Hokke, J.F.G. Vliegenhart, P. Kamerling, H.S. Conradt, M. Nimtz and D. Brazel, *Anal. Biochem.*, 221 (1994) 29.